

Library Copy
B.A. 1507

Copy No. 44
RM No. SL8K10

Inactive

NACA

RESEARCH MEMORANDUM

for the

Air Materiel Command, U. S. Air Force

A THEORETICAL INVESTIGATION OF THE DYNAMIC LATERAL STABILITY

CHARACTERISTICS OF THE MX-838 (XB-51) AIRPLANE

By

John W. Paulson

Langley Aeronautical Laboratory
Langley Field, Va.

CLASSIFIED DOCUMENT

This document contains classified information affecting the National Defense of the United States within the meaning of the Espionage Act, USC 50:31 and 32. Its transmission or the revelation of its contents in any manner to an unauthorized person is prohibited by law. Information so classified may be imparted only to persons in the military and naval services of the United States, appropriate civilian officers and employees of the Federal Government who have a legitimate interest therein, and to United States citizens of known loyalty and discretion and of necessity must be informed thereof.

NATIONAL ADVISORY COMMITTEE
FOR AERONAUTICS
WASHINGTON

CLASSIFICATION CANCELLED

Authority 12 3142 Date 12/4/55

See 12/4/55

12/4/55
CLASSIFIED DOCUMENT
LANGLEY FIELD



NATIONAL ADVISORY COMMITTEE FOR AERONAUTICS

RESEARCH MEMORANDUM

for the

Air Materiel Command, U. S. Air Force

A THEORETICAL INVESTIGATION OF THE DYNAMIC LATERAL STABILITY

CHARACTERISTICS OF THE MX-838 (XB-51) AIRPLANE

By John W. Paulson

SUMMARY

At the request of the Air Materiel Command, U. S. Air Force, a theoretical study has been made of the dynamic lateral stability characteristics of the MX-838 (XB-51) airplane. The calculations included the determination of the neutral-oscillatory-stability boundary ($R = 0$), the period and time to damp to one-half amplitude of the lateral oscillation, and the time to damp to one-half amplitude for the spiral mode. Factors varied in the investigation were lift coefficient, wing incidence, wing loading, and altitude.

The results of the investigation showed that the lateral oscillation of the airplane is unstable below a lift coefficient of 1.2 with flaps deflected 40° but is stable over the entire speed range with flaps deflected 20° or 0° . The results showed that satisfactory oscillatory stability can probably be obtained for all lift coefficients with the proper variation of flap deflection and wing incidence with airspeed. Reducing the positive wing incidence improved the oscillatory stability characteristics. The airplane is spirally unstable for most conditions but the instability is mild and the Air Force requirements are easily met.

INTRODUCTION

At the request of the Air Materiel Command, U. S. Air Force, a theoretical study has been made of the dynamic lateral stability characteristics of the MX-838 (XB-51) airplane. A three-view sketch of the airplane is shown in figure 1. The calculations were made at the Langley Laboratory on the Bell Telephone Laboratory's X-66744 relay computer. The analysis was made by the Langley free-flight-tunnel staff.

20-5886-1

Calculations were made to determine the neutral-lateral-oscillatory-stability boundary ($R = 0$), the period and time to damp to one-half amplitude of the lateral oscillation, and the time to damp to one-half amplitude for the spiral mode for several conditions of the airplane. The factors varied included lift coefficient, wing incidence, wing loading, and altitude. The results of the investigation are presented in the form of stability charts where the $R = 0$ boundaries are plotted as functions of the effective-dihedral parameter $-C_{l\beta}$ and the directional-stability parameter $C_{n\beta}$.

The period and time to damp to one-half amplitude are presented as functions of lift coefficient for the various conditions investigated.

SYMBOLS AND COEFFICIENTS

S	wing area, square feet
\bar{c}	mean aerodynamic chord, feet
V	airspeed, feet per second
b	wing span, feet
q	dynamic pressure, pounds per square foot
ρ	air density, slugs per cubic foot
W	weight, pounds
g	acceleration of gravity, feet per second per second
m	mass, slugs (W/g)
μ_b	relative-density factor based on wing span ($m/\rho S b$)
i_w	wing incidence, degrees
α	angle of attack of reference axis (fig. 2), degrees
η	angle of attack of principal longitudinal axis of airplane, positive when principal axis is above flight path at the nose (fig. 2), degrees
ϵ	angle between reference axis and principal axis, positive when reference axis is above principal axis at the nose (fig. 2), degrees
θ	angle between reference axis and horizontal axis, positive when reference axis is above horizontal axis at the nose (fig. 2), degrees

γ	angle of flight to horizontal axis, positive in a climb (fig. 2), degrees
ψ	angle of yaw, degrees or radians
β	angle of sideslip, degrees or radians
ϕ	angle of bank, radians
R	Routh's discriminant ($R = BCD - AD^2 - B^2E$ where A , B , C , D , and E are constants representing coefficients of the lateral-stability equation)
k_{X_0}	radius of gyration about principal longitudinal axis, feet
k_{Z_0}	radius of gyration about principal vertical axis, feet
K_{X_0}	nondimensional radius of gyration about principal longitudinal axis (k_{X_0}/b)
K_{Z_0}	nondimensional radius of gyration about principal vertical axis (k_{Z_0}/b)
K_X	nondimensional radius of gyration about longitudinal stability axis $\left(\sqrt{K_{X_0}^2 \cos^2 \eta + K_{Z_0}^2 \sin^2 \eta}\right)$
K_Z	nondimensional radius of gyration about vertical stability axis $\left(\sqrt{K_{Z_0}^2 \cos^2 \eta + K_{X_0}^2 \sin^2 \eta}\right)$
K_{XZ}	nondimensional product-of-inertia parameter $\left((K_{Z_0}^2 - K_{X_0}^2) \cos \eta \sin \eta\right)$
C_L	lift coefficient (Lift/ qS)
C_n	yawing-moment coefficient (Yawing moment/ qSb)
C_l	rolling-moment coefficient (Rolling moment/ qSb)
C_Y	lateral-force coefficient (Lateral force/ qS)
$C_{Y\beta}$	rate of change of lateral-force coefficient with angle of sideslip, per degree or per radian, as specified $(\partial C_Y / \partial \beta)$

$C_{n\beta}$	rate of change of yawing-moment coefficient with angle of sideslip, per degree or per radian, as specified $\left(\frac{\partial C_n}{\partial \beta}\right)$
$C_{l\beta}$	rate of change of rolling-moment coefficient with angle of sideslip, per degree or per radian, as specified $\left(\frac{\partial C_l}{\partial \beta}\right)$
C_{Yp}	rate of change of lateral-force coefficient with rolling-angular-velocity factor, per radian $\left(\frac{\partial C_Y}{\frac{\partial pb}{2V}}\right)$
C_{lp}	rate of change of rolling-moment coefficient with rolling-angular-velocity factor, per radian $\left(\frac{\partial C_l}{\frac{\partial pb}{2V}}\right)$
C_{np}	rate of change of yawing-moment coefficient with rolling-angular-velocity factor, per radian $\left(\frac{\partial C_n}{\frac{\partial pb}{2V}}\right)$
C_{lr}	rate of change of rolling-moment coefficient with yawing-angular-velocity factor, per radian $\left(\frac{\partial C_l}{\frac{\partial rb}{2V}}\right)$
C_{nr}	rate of change of yawing-moment coefficient with yawing-angular-velocity factor, per radian $\left(\frac{\partial C_n}{\frac{\partial rb}{2V}}\right)$
C_{Yr}	rate of change of lateral-force coefficient with yawing-angular-velocity factor, per radian $\left(\frac{\partial C_Y}{\frac{\partial rb}{2V}}\right)$
l	tail length (distance from center of gravity to rudder hinge line), feet
\bar{z}	height of center of pressure of vertical tail above fuselage axis, feet

p	rolling angular velocity, radians per second
r	yawing angular velocity, radians per second
D_b	differential operator (d/ds_b)
s_b	distance along flight path, spans (Vt/b)
λ	complex root of stability equation $(c \pm id)$
t	time, seconds
P	period of oscillation, seconds
$T_{1/2}$	time for amplitude of oscillation or spiral mode to change by factor of 2 (positive value indicates a decrease to half-amplitude, negative value indicates an increase to double amplitude)
$C_{1/2}$	cycles for amplitude of oscillation to change by a factor of 2

EQUATIONS OF MOTION

The nondimensional lateral equations of motion (reference 1), referred to a stability-axes system (fig. 3), are:

Roll

$$2\mu_b(K_X^2 D_b^2 \phi + K_{XZ} D_b^2 \psi) = C_{L\beta} \beta + \frac{1}{2} C_{Lp} D_b \phi + \frac{1}{2} C_{Lr} D_b \psi$$

Yaw

$$2\mu_b(K_Z^2 D_b^2 \psi + K_{XZ} D_b^2 \phi) = C_{n\beta} \beta + \frac{1}{2} C_{np} D_b \phi + \frac{1}{2} C_{nr} D_b \psi$$

Sideslip

$$2\mu_b(D_b \beta + D_b \psi) = C_{Y\beta} \beta + \frac{1}{2} C_{Yp} D_b \phi + C_{L\phi} \phi + \frac{1}{2} C_{Yr} D_b \psi + (C_{L\phi} \tan \gamma) \psi$$

When $\phi_0 e^{\lambda s_b}$ is substituted for ϕ , $\psi_0 e^{\lambda s_b}$ for ψ , and $\beta_0 e^{\lambda s_b}$ for β in the equations written in determinant form, λ must be a root of the stability equation

$$A\lambda^4 + B\lambda^3 + C\lambda^2 + D\lambda + E = 0$$

where

$$A = -b^3(K_X^2 K_Z^2 - K_{XZ}^2)$$

$$B = -2\mu_b^2(2K_X^2 K_Z^2 C_{Y\beta} + K_X^2 C_{n_r} + K_Z^2 C_{l_p} - 2K_{XZ}^2 C_{Y\beta} - K_{XZ} C_{l_r} - K_{XZ} C_{n_p})$$

$$C = \mu_b(K_X^2 C_{n_r} C_{Y\beta} + 4\mu_b K_X^2 C_{n\beta} + K_Z^2 C_{l_p} C_{Y\beta} + \frac{1}{2} C_{n_r} C_{l_p} - K_{XZ} C_{l_r} C_{Y\beta} \\ - 4\mu_b K_{XZ} C_{l\beta} - C_{n_p} K_{XZ} C_{Y\beta} - \frac{1}{2} C_{n_p} C_{l_r} + K_{XZ} C_{n\beta} C_{Y_p} \\ - K_Z^2 C_{Y_p} C_{l\beta} - K_X^2 C_{Y_r} C_{n\beta} + K_{XZ} C_{Y_r} C_{l\beta})$$

$$D = -\frac{1}{4} C_{n_r} C_{l_p} C_{Y\beta} - \mu_b C_{l_p} C_{n\beta} + \frac{1}{4} C_{n_p} C_{l_r} C_{Y\beta} + \mu_b C_{n_p} C_{l\beta} \\ + 2\mu_b C_L K_{XZ} C_{n\beta} - 2\mu_b C_L K_Z^2 C_{l\beta} - 2\mu_b K_X^2 C_{n\beta} C_L \tan \gamma \\ + 2\mu_b K_{XZ} C_{l\beta} C_L \tan \gamma + \frac{1}{4} C_{l_p} C_{n\beta} C_{Y_r} - \frac{1}{4} C_{n_p} C_{l\beta} C_{Y_r} - \frac{1}{4} C_{l_r} C_{n\beta} C_{Y_p} \\ + \frac{1}{4} C_{n_r} C_{l\beta} C_{Y_p}$$

$$E = \frac{1}{2} C_L (C_{n_r} C_{l\beta} - C_{l_r} C_{n\beta}) + \frac{1}{2} C_L \tan \gamma (C_{l_p} C_{n\beta} - C_{n_p} C_{l\beta})$$

The damping and period of the lateral oscillation are given by the equations $T_{1/2} = -\frac{0.69}{c} \frac{b}{V}$, $P = \frac{2\pi}{d} \frac{b}{V}$ and $C_{1/2} = \frac{T_{1/2}}{P}$ where c and d are the real and imaginary parts of the complex root of the stability equation. The damping of the spiral mode is determined similarly from one of the two real roots (usually the less stable one) of the stability equation.

The conditions for neutral oscillatory stability as shown in reference 2 are that the coefficients of the stability equation satisfy Routh's discriminant set equal to zero

$$R = BCD - AD^2 - B^2E = 0$$

and that the coefficients B and D have the same sign. In general, the sign of the coefficient B is determined by the factors $-C_{Y\beta}$, $-C_{n_r}$, and $-C_{l_p}$ which appear in the predominant terms of B . Thus, B is positive in the usual case if there is positive weathercock stability and positive damping

in roll. Hence, the coefficient D must be positive if $R = 0$ is a neutral-oscillatory-stability boundary.

SCOPE OF THE CALCULATIONS

Calculations were made of the neutral-oscillatory-stability boundary, the period and time to damp to one-half amplitude for the lateral oscillation, and the time to damp to one-half amplitude for the spiral mode for several conditions of the airplane. The effect of lift coefficient was determined for flaps deflected and retracted for weights of 53,000 and 32,017 pounds. The effect of varying wing incidence from 9° to 2° and -5.3° was also determined for a weight of 32,017 pounds with flaps deflected and the effect of changing altitude from sea level to 35,000 feet was determined for flaps up at a weight of 53,000 pounds.

The aerodynamic and mass characteristics used in the calculation of the boundaries are presented in table I. The values of $(C_{n\beta})_{\text{tail off}}$ and $(C_{Y\beta})_{\text{tail off}}$ were obtained from force-test data furnished by the Glenn L. Martin Company. The tail-off values of C_{L_p} , C_{n_p} , C_{L_r} , C_{n_r} , and C_{Y_p} were estimated from data obtained in the Langley stability tunnel on a wing similar to that of the MX-838 airplane. The total derivatives including the contribution of the tail were estimated from the equations presented with table I.

The roots of the stability equation were computed to determine the period and time to damp to one-half amplitude for each condition for which a boundary was calculated. Presented in table II are the aerodynamic and mass characteristics used in computing the roots of the stability equations. The values are essentially the same as those given in table I except that the mass characteristics are presented in a different form and the total derivatives are given. The values of $C_{n\beta}$ and $-C_{L\beta}$ used in these calculations were obtained from force-test data furnished by the Glenn L. Martin Company.

The variation of these values with flap deflection is shown in the following table:

δ_f (deg)	$C_{n\beta}$ (per deg)	$-C_{L\beta}$ (per deg)
40	0.00523	0.00400
20	.00490	.00290
0	.00454	.00175

These values were assumed to remain constant with lift coefficient for a given configuration of the airplane on the basis of the force-test results available on a model of this airplane. It would be expected, however, that the airplane would show an increase in $-C_{l\beta}$ at the higher lift coefficients.

RESULTS AND DISCUSSION

The results of the calculations are presented in figures 4 to 16. All results are presented in terms of lift coefficient and figure 14 is presented for convenience in interpreting the results in terms of airspeed. The test point in figures 4 to 9 represents the C_{np} and $-C_{l\beta}$ values of the airplane as shown by force-test results.

Neutral-Oscillatory-Stability Boundaries

Flaps down 40°. - The effect of lift coefficient is shown in figure 4(a) for the airplane with flaps down at sea level, $i_w = 9^\circ$, and a weight of 53,000 pounds. It is seen that the airplane is oscillatorily unstable below a lift coefficient of 1.2 and becomes stable at lift coefficients above this value. The results of figure 4(b) are for the same condition as figure 4(a) except that the weight is 32,017 pounds. Here again the airplane is unstable below $C_L = 1.2$ and stable at higher values.

The effect of wing incidence on the lateral stability of the airplane is shown in figure 5 for a lift coefficient of 0.4 with flaps down, light loading, and sea-level condition. Changing the wing incidence from 9° to 2° has a relatively small effect on the boundary although it is shifted downward far enough to make the airplane slightly stable. A further change in wing incidence to -5.3° (this change brought the inclination of the principal longitudinal axis of inertia with respect to the flight path to 0°) resulted in the airplane being very stable. The small shift in the boundary occasioned by the incidence change from 9° to 2° can be accounted for by the fact that with this change the principal axis of inertia was moved from -14.3° to -7.3° . Previous investigations (reference 3) have shown that the greatest effect of changes in the principal axis occurs at angles around 0° . Thus, when the incidence was changed so as to bring the principal axis from -7.3 to 0° , a large downward shift in the $R = 0$ boundary was obtained.

Flaps down 20°. - The effect of lift coefficient on the $R = 0$ boundary for the airplane at sea level, half flap, $i_w = 5.5^\circ$, and 53,000 pounds is shown in figure 6(a). The boundaries for a weight of 32,017 pounds are given in figure 6(b). From these results it is seen that the oscillation of the airplane is stable at $C_L = 0.4$ and the stability increases with increasing lift coefficient.

Flaps up.- The effect of lift coefficient on the oscillatory stability of the airplane with flaps retracted at sea level, $i_w = 2^\circ$, and a weight of 53,000 pounds is shown in figure 7(a). The airplane appears to have satisfactory stability even at a lift coefficient of 0.1 and increasing the lift coefficient resulted in a pronounced increase in stability. The results of the calculations made to determine the stability characteristics of the airplane with flaps up at 35,000 feet are presented in figure 7(b). These results show the same general effect of lift coefficient as for the sea-level condition.

The results presented in figure 8 show the effect of a change in wing incidence from 2° to 0° for the flap-retracted condition at an altitude of 35,000 feet and a weight of 53,000 pounds. The 2° incidence change resulted in a fairly large downward shift in the boundary because of the fact that the change in the principal axis occurred near 0° (-3.4° to -1.4°).

Modified airplane.- A boundary was calculated for the airplane with flaps deflected 40° to determine the effect of several mass and geometric changes proposed by the Glenn L. Martin Company. The maximum wing incidence was assumed to be 7° instead of 9° , the tail length was increased 59 inches by moving the vertical tail to the rear of the fuselage, the negative dihedral was increased from -3° to -6° , and the inclination of the principal longitudinal axis of inertia was assumed to be -4° instead of -3° . The calculations were made for a weight of 40,200 pounds and a full-flap placard speed of 165 miles per hour which corresponds to a lift coefficient of 1.05. The results of these calculations are presented in figure 9(a). In order to show the effect of these changes a boundary is presented in figure 9(b) which was obtained by interpolating between the flap-down results of figures 4(a) and 4(b). The results of figure 9(a) show that the geometric and mass changes caused the airplane to have a small degree of oscillatory stability, whereas in the original condition (fig. 9(b)) it was slightly unstable. The modifications had very little effect on the boundary and the improved stability was due primarily to a change in $C_{n\beta}$ and $-C_{l\beta}$ which shifted the airplane point with respect to the boundary.

Period and Damping of the Lateral Oscillation

The period of the lateral oscillation as a function of lift coefficient is presented in figure 10 for the various conditions investigated. It is seen that the period increases rather rapidly as the lift coefficient is increased from low to moderate values and increases at a lesser rate at the higher lift coefficients. For a given lift coefficient the period increases slightly as the flap deflection is increased and the period is greatest for the light loading. There is very little effect of altitude at low lift coefficients and at higher lift coefficients increasing altitude results in a slight decrease in the period.

The reciprocal of the time to damp to one-half amplitude is plotted as a function of lift coefficient in figure 11. The larger values of the factor $\frac{1}{T_{1/2}}$ indicate the greater damping. It is seen from this figure that the time to damp is negative below $C_L = 1.2$ with flaps deflected 40° , which indicates instability for the airplane; whereas, the damping is positive for the 20° and 0° flap conditions. The effect of changing wing incidence from 9° to 2° and -5.3° at $C_L = 0.4$ is shown for the 40° flap condition. These changes would make the airplane stable although the damping is still probably unsatisfactory with 2° wing incidence. The damping increases with lift coefficient for 40° and 20° flap conditions with the greatest change occurring with the heavy loading. With flaps retracted the damping decreases in going from $C_L = 0.1$ to $C_L = 0.4$ and then increases at lift coefficients beyond 0.4. The damping was relatively high, however, at all lift coefficients. The flap-retracted condition also shows that the effect of going from sea level to 35,000 feet resulted in a large decrease in the damping although the airplane was still quite stable.

Perhaps a clearer picture of the results of the investigation is shown in figure 12 where the reciprocal of the cycles to damp to one-half amplitude is plotted as a function of lift coefficient. The cycles to damp are determined by dividing the time to damp by the period. If the value of $\frac{1}{C_{1/2}}$ is greater than 0.5, it means that the lateral oscillation damps in two cycles or less. From figure 12 it is seen that with flaps up, all conditions damp in two cycles or less; whereas with flaps down 40° , only the heavy loading at the highest lift coefficients damps in two cycles. The low-lift-coefficient conditions with flaps up and an altitude of 35,000 feet are actually impossible to attain with this airplane because of the high speed required as shown in figure 13.

From the results presented it is seen that there is a range of lift coefficients for oscillatory stability for the airplane for all flap conditions even though the range becomes quite small with a flap deflection of 40° . If care is taken to insure that the airspeed is low enough before a given flap deflection is reached, then the dynamic lateral stability might be satisfactory over the entire speed range. One suggested means for insuring the proper flap setting with airspeed has been an automatic flap-unloading device. This device would allow flap deflection and wing incidence to change with airspeed such that a stable condition was always maintained. Figure 14 has been prepared to show how such a flap-unloading device might be applied. The reciprocal of the cycles to damp to one-half amplitude has been plotted as a function of airspeed in miles per hour for flap deflections of 0° , 10° , 20° , 30° , and 40° . (The curves for 10° and 30° flap deflections were obtained by interpolation.) A linear variation of flap deflection with airspeed was assumed and cross-plotted as dashed curves in figure 14 to show the damping of the airplane for

each flap position. The lower of the two curves is based on the assumption that the flap is released at 250 miles per hour and reaches full deflection at 165 miles per hour whereas the upper curve was based on a flap release speed of 220 miles per hour and a full-flap speed of 155 miles per hour. It is seen that the airplane remains stable for all conditions although the oscillation requires more than two cycles to damp with 40° flap deflection at a speed of 165 miles per hour. This damping might not be objectionable in the landing condition and a reduction in speed to 150 miles per hour would bring the oscillation to a two-cycle damping.

The fact that the lateral oscillation damps in two cycles does not necessarily indicate that the lateral stability is satisfactory. Some present-day airplanes when flying at high speeds have encountered undesirable short-period oscillations that damp in less than two cycles. The Air Force and Navy have therefore set up requirements which call for greater damping of the shorter-period oscillations. Presented in figure 15 is a plot showing how the MX-838 airplane damping compares with the requirements of both the Air Force and NACA. (See references 4 and 5.) It is seen that the Air Force requirement is much more stringent than the NACA requirement for periods from 1 to 3 seconds. Figure 15 shows that several conditions of the airplane that meet the NACA requirement would actually be unsatisfactory or very close to being marginal when considering the Air Force requirement.

Spiral Stability

The reciprocal of the time to damp to one-half amplitude for the spiral motion is presented in figure 16 for all conditions investigated. It is seen that most conditions are spirally unstable but the instability is not severe. In all cases the spiral instability increases up to a lift coefficient of about 0.8 and then decreases at higher lift coefficients.

Although neither the Air Force nor the NACA flying-qualities requirements call for spiral stability, they do require that any spiral instability present should be mild. The Air Force requirement is for the spiral motion not to double amplitude in less than 4 seconds. It is seen from figure 16 that the spiral instability of the MX-838 airplane will be acceptable for all conditions.

CONCLUSIONS

The following conclusions are drawn from the results of the theoretical study of the dynamic lateral stability characteristics of the MX-838 airplane:

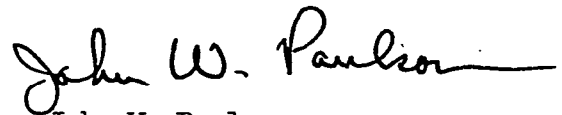
1. The lateral oscillation of the airplane is unstable below a lift coefficient of about 1.2 with the flaps deflected 40° but is stable over

the entire speed range with flap deflections of 20° or 0° . Satisfactory oscillatory stability can probably be obtained for all lift coefficients with the proper variation of flap deflection and wing incidence with airspeed.

2. Reducing the wing incidence from 9° to 2° with flaps deflected 40° makes the lateral oscillation of the airplane slightly stable. A further change in wing incidence to -5.3° (this change brought the inclination of the principal axis to 0°) results in the airplane being very stable.

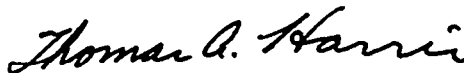
3. The airplane is spirally unstable for most conditions but the instability is mild and the Air Force requirements are easily met.

Langley Aeronautical Laboratory
National Advisory Committee for Aeronautics
Langley Field, Va.



John W. Paulson
Aeronautical Research Scientist

Approved:



Thomas A. Harris
Chief of Stability Research Division

DLMc

REFERENCES

1. Sternfield, Leonard: Some Considerations of the Lateral Stability of High-Speed Aircraft. NACA TN No. 1282, 1947.
2. Routh, Edward John: Dynamics of a System of Rigid Bodies. Pt. II. Macmillan and Company, Ltd., 1930.
3. Sternfield, Leonard, and McKinney, Marion O., Jr.: Dynamic Lateral Stability as Influenced by Mass Distribution. Jour. Aero. Sci. vol. 15, no. 7, pp. 411-417, July 1948.
4. Gilruth, R. R.: Requirements for Satisfactory Flying Qualities of Airplanes. NACA Rep. No. 755, 1943.
5. Anon.: Flying Qualities of Piloted Airplanes. U. S. Air Force Specification No. 1815-B, June 1, 1948.

~~CONFIDENTIAL~~
TABLE I

FACTORS USED IN CALCULATING THE OSCILLATORY STABILITY BOUNDARIES

Flap deflection (deg)	C_L	α (deg)	η (deg)	i_w (deg)	W (lb)	ρ (slugs/cu ft)	μ_b	k_{x_0}	k_{z_0}	$(C_{Y\beta})_{tail\ off}$	$(C_{n\beta})_{tail\ off}$	$(C_{l\beta})_{tail\ off}$	$(C_{n\beta})_{tail\ off}$	$(C_{l_r})_{tail\ off}$	$(C_{n_r})_{tail\ off}$
40	0.4	-11.3	-14.3	9	53,000	0.002378	23.6	5.37	16.5	-0.57	-0.074	-0.35	-0.05	0.22	-0.125
	.8	-6.1	-9.1	9	53,000	.002378	23.6	5.37	16.5	-.57	-.074	-.35	-.05	.32	-.15
	1.2	-.9	-3.9	9	53,000	.002378	23.6	5.37	16.5	-.57	-.074	-.35	-.05	.35	-.175
	1.6	4.3	1.3	9	53,000	.002378	23.6	5.37	16.5	-.57	-.074	-.35	-.05	.35	-.20
	.4	-11.3	-14.3	9	32,017	.002378	14.27	6.56	20.0	-.57	-.074	-.35	-.05	.22	-.125
	.8	-6.1	-9.1	9	32,017	.002378	14.27	6.56	20.0	-.57	-.074	-.35	-.05	.32	-.15
	1.2	-.9	-3.9	9	32,017	.002378	14.27	6.56	20.0	-.57	-.074	-.35	-.05	.35	-.175
	1.6	4.3	1.3	9	32,017	.002378	14.27	6.56	20.0	-.57	-.074	-.35	-.05	.35	-.20
	.4	-4.3	-7.3	2	32,017	.002378	14.27	6.56	20.0	-.57	-.074	-.35	-.05	.22	-.125
	.4	3.0	0	-5.3	32,017	.002378	14.27	6.56	20.0	-.57	-.074	-.35	-.05	.22	-.125
	1.05	-.8	-4.8	7	40,200	.002378	17.9	6.02	18.6	-.57	-.074	-.35	-.05	.34	-.166
	.4	-3.8	-6.8	5.5	53,000	.002378	23.6	5.37	16.5	-.45	-.11	-.35	-.05	.18	-.075
20	.8	1.5	-1.5	5.5	53,000	.002378	23.6	5.37	16.5	-.45	-.11	-.35	-.05	.28	-.095
	1.2	6.9	3.9	5.5	53,000	.002378	23.6	5.37	16.5	-.45	-.11	-.35	-.05	.30	-.11
	.4	-3.8	-4.8	5.5	53,000	.002378	14.27	6.56	20.0	-.45	-.11	-.35	-.05	.18	-.075
	.8	1.5	-1.5	5.5	32,017	.002378	14.27	6.56	20.0	-.45	-.11	-.35	-.05	.28	-.095
	1.2	6.9	3.9	5.5	32,017	.002378	14.27	6.56	20.0	-.45	-.11	-.35	-.05	.30	-.11
	.1	-.4	-3.4	2	53,000	.002378	23.6	5.37	16.5	-.34	-.15	-.35	-.05	0	-.015
	.4	3.8	.8	2	53,000	.002378	23.6	5.37	16.5	-.34	-.15	-.35	-.05	.15	-.025
	.8	9.2	6.2	2	53,000	.002378	23.6	5.37	16.5	-.34	-.15	-.35	-.05	.24	-.035
	1.2	15.0	12.0	2	53,000	.002378	23.6	5.37	16.5	-.34	-.15	-.35	-.05	.25	-.05
	.1	-.4	-3.4	2	53,000	.000736	76.3	5.37	16.5	-.34	-.15	-.35	-.05	0	-.015
	.4	3.8	.8	2	53,000	.000736	76.3	5.37	16.5	-.34	-.15	-.35	-.05	.15	-.025
	.8	9.2	6.2	2	53,000	.000736	76.3	5.37	16.5	-.34	-.15	-.35	-.05	.24	-.035
0	1.2	15.0	12.0	2	53,000	.000736	76.3	5.37	16.5	-.34	-.15	-.35	-.05	.25	-.05
	.1	1.6	-1.4	0	53,000	.000736	76.3	5.37	16.5	-.34	-.15	-.35	-.05	0	-.015



Constants:

$b = 53.3$ ft
 $S = 550$ sq ft
 $\gamma = 0^\circ$

$\frac{l}{b} = 0.58$ ft (0.67 ft used for $C_L = 1.05$ condition)
 $y_p = 0$

Variables:

$(C_{Y\beta})_{tail} = 0.2$ to -1.0
 $\frac{z}{b} = 0.08$ to 0.185

Total derivatives including tail contributions are determined from the following equations:

$$\begin{aligned}
 (C_{Y\beta})_{C_{n\beta}=0} &= -0.35 - 2\left(\frac{z}{b} - \frac{l}{b} \sin \alpha\right)^2 \frac{b}{l} (-C_{n\beta})_{tail\ off} & (C_{Y\beta})_{total} &= (C_{Y\beta})_{C_{n\beta}=0} - 2\left(\frac{z}{b} - \frac{l}{b} \sin \alpha\right)^2 \frac{b}{l} C_{n\beta} \\
 (C_{l_r})_{C_{n\beta}=0} &= (C_{l_r})_{tail\ off} + 2\left(\frac{z}{b} - \frac{l}{b} \sin \alpha\right) (-C_{n\beta})_{tail\ off} & (C_{l_r})_{total} &= (C_{l_r})_{C_{n\beta}=0} + 2\left(\frac{z}{b} - \frac{l}{b} \sin \alpha\right) C_{n\beta} \\
 (C_{n\beta})_{C_{n\beta}=0} &= -0.05 + 2\left(\frac{z}{b} - \frac{l}{b} \sin \alpha\right) (-C_{n\beta})_{tail\ off} & (C_{n\beta})_{total} &= (C_{n\beta})_{C_{n\beta}=0} + 2\left(\frac{z}{b} - \frac{l}{b} \sin \alpha\right) C_{n\beta} \\
 (C_{n_r})_{C_{n\beta}=0} &= (C_{n_r})_{tail\ off} - 2\frac{l}{b} (-C_{n\beta})_{tail\ off} & (C_{n_r})_{total} &= (C_{n_r})_{C_{n\beta}=0} - 2\left(\frac{l}{b} C_{n\beta}\right)
 \end{aligned}$$

TABLE II

FACTORS USED IN CALCULATING ROOTS OF LATERAL-STABILITY EQUATIONS FOR DETERMINATION OF PERIOD AND TIME TO DAMP

Flap deflection (deg)	C_L	η (deg)	μ_b	$\left(\frac{k_{X_0}}{b}\right)^2$	$\left(\frac{k_{Z_0}}{b}\right)^2$	K_X^2	K_Z^2	K_{XZ}	$(C_{l_p})_{total}$	$(C_{Y_p})_{total}$	$(C_{l_r})_{total}$	$(C_{n_p})_{total}$	$(C_{n_r})_{total}$	$\frac{m}{\rho S V}$
40	0.4	-14.3	23.6	0.0102	0.0958	0.0154	0.0906	-0.0180	-0.4466	-1.15	0.4247	0.1547	-0.5588	2.8
	.8	-9.1	23.6	0.0102	0.0958	0.0123	0.0937	-0.0127	-0.4134	-1.15	.4858	.1158	-.5838	3.94
	1.2	-3.9	23.6	0.0102	0.0958	0.0106	0.0954	-0.0058	-.3869	-1.15	.4765	.0765	-.6088	4.85
	1.6	1.3	23.6	0.0102	0.0958	0.0102	0.0957	.0019	-.3675	-1.15	.4371	.0371	-.6338	5.60
	.4	-14.3	14.27	0.0151	.1408	.0228	.1331	-.0264	-.4466	-1.15	.4247	.1547	-.5588	2.17
	.8	-9.1	14.27	0.0151	.1408	.0182	.1377	-.0187	-.4134	-1.15	.4858	.1158	-.5838	3.06
	1.2	-3.9	14.27	0.0151	.1408	.0156	.1403	-.0085	-.3869	-1.15	.4765	.0765	-.6088	3.76
	1.6	1.3	14.27	0.0151	.1408	.0152	.1407	.0028	-.3675	-1.15	.4371	.0371	-.6338	4.35
	.4	-7.3	14.27	0.0151	.1408	.0172	.1387	-.0153	-.4035	-1.15	.3170	.1022	-.5588	2.17
	.4	0	14.27	0.0151	.1408	.0151	.1408	0	-.3717	-1.15	.3346	.0470	-.5588	2.17
	1.05	-4.8	17.9	0.0128	.1218	.0136	.1210	-.0090	-.3869	-1.15	.4861	.096	-.744	3.94
	.4	-6.8	23.6	0.0102	0.0958	0.0114	0.0946	-.0098	-.4031	-1.10	.3346	.1046	-.5275	2.8
20	.8	-1.5	23.6	0.0102	0.0958	0.0103	0.0947	-.0022	-.3782	-1.10	.3928	.0628	-.5475	3.94
	1.2	3.9	23.6	0.0102	0.0958	0.0106	0.0954	.0058	-.3610	-1.10	.3705	.0205	-.5625	4.85
	.4	-6.8	14.27	0.0151	.1408	.0169	.1390	-.0144	-.4031	-1.10	.3346	.1046	-.5275	2.17
	.8	-1.5	14.27	0.0151	.1408	.0152	.1407	-.0033	-.3782	-1.10	.3928	.0628	-.5475	3.06
	1.2	3.9	14.27	0.0151	.1408	.0156	.1403	.0085	-.3610	-1.10	.3705	.0205	-.5625	3.76
	.1	-3.4	23.6	0.0102	0.0958	0.0105	0.0956	-.0050	-.3881	-1.05	.1345	.0845	-.4906	1.395
	.4	.8	23.6	0.0102	0.0958	0.0102	0.0959	.0012	-.3708	-1.05	.2496	.0496	-.5006	2.80
	.8	6.2	23.6	0.0102	0.0958	0.0112	0.0949	.0090	-.3564	-1.05	.2952	.0052	-.5106	3.94
	1.2	12.0	23.6	0.0102	0.0958	0.0139	0.0921	.0159	-.3502	-1.05	.2581	-.0419	-.5256	4.85
	.1	-3.4	76.3	0.0102	0.0958	0.0105	0.0956	-.0050	-.3881	-1.05	.1345	.0845	-.4906	2.51
	.4	.8	76.3	0.0102	0.0958	0.0102	0.0959	.0012	-.3708	-1.05	.2496	.0496	-.5006	5.02
	.8	6.2	76.3	0.0102	0.0958	0.0112	0.0949	.0090	-.3564	-1.05	.2952	.0052	-.5106	7.10
0	1.2	12.0	76.3	0.0102	0.0958	0.0139	0.0921	.0159	-.3502	-1.05	.2581	-.0419	-.5256	8.69
	.1	-1.4	76.3	0.0102	0.0958	0.0103	0.0958	-.0021	-.3792	-1.05	.1179	.0679	-.4906	2.51

Constants:

$$C_{Y_p} = 0$$

$$C_{Y_r} = 0$$

$$\gamma = 0^\circ$$

~~CONFIDENTIAL~~

NACA



Figure 1.- Three-view drawing of the MX-838 (XB-51) airplane.

~~CONFIDENTIAL~~

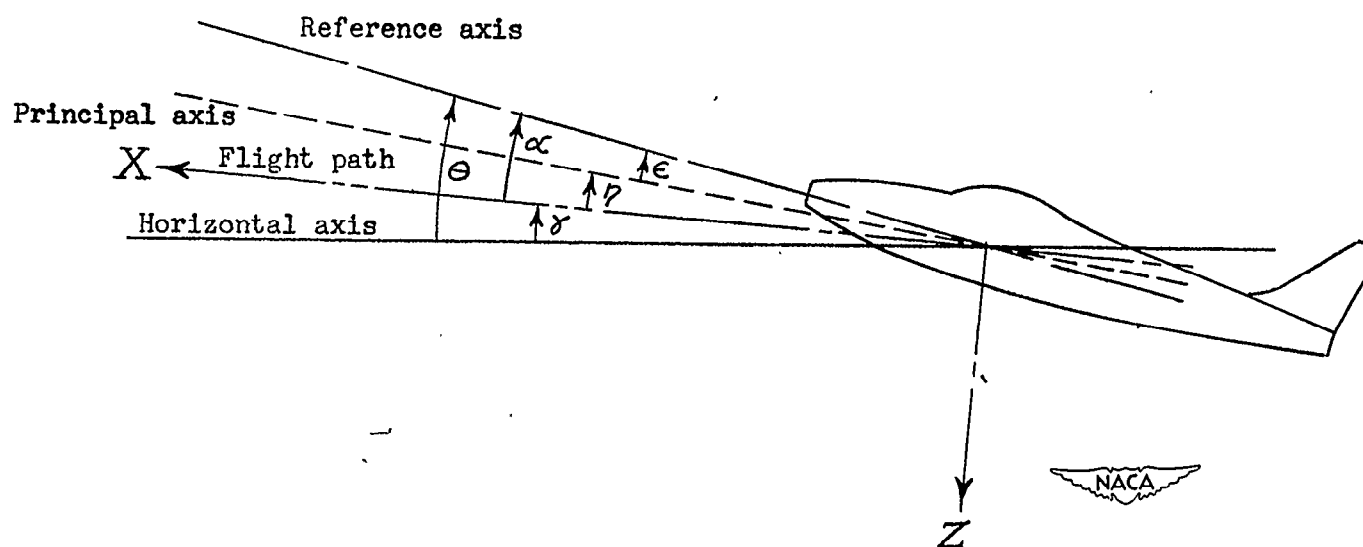


Figure 2.— System of axes and angular relationship in flight. Arrows indicate positive direction of angles. $\eta = \theta - \gamma - \epsilon$.

~~CONFIDENTIAL~~

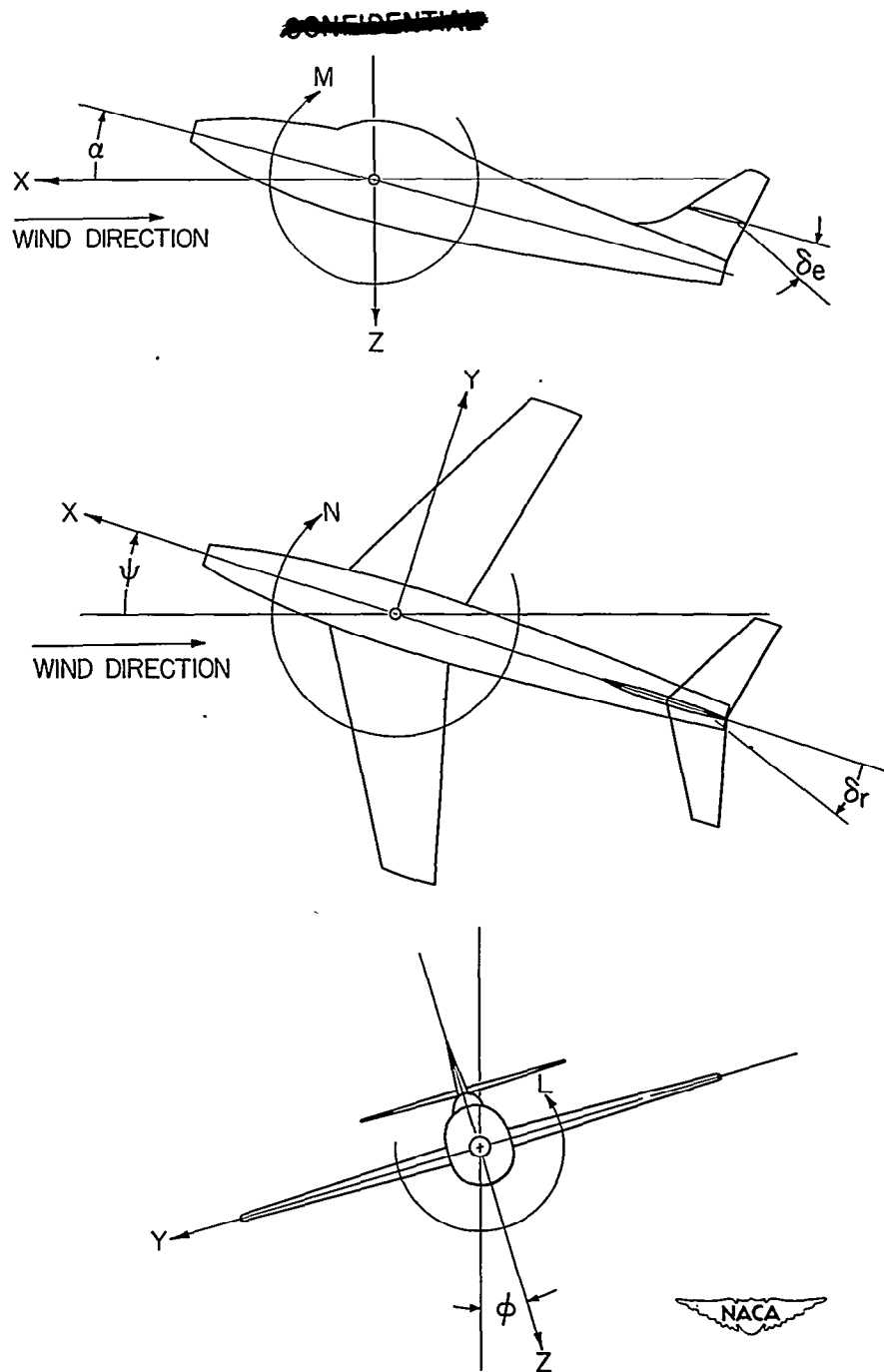
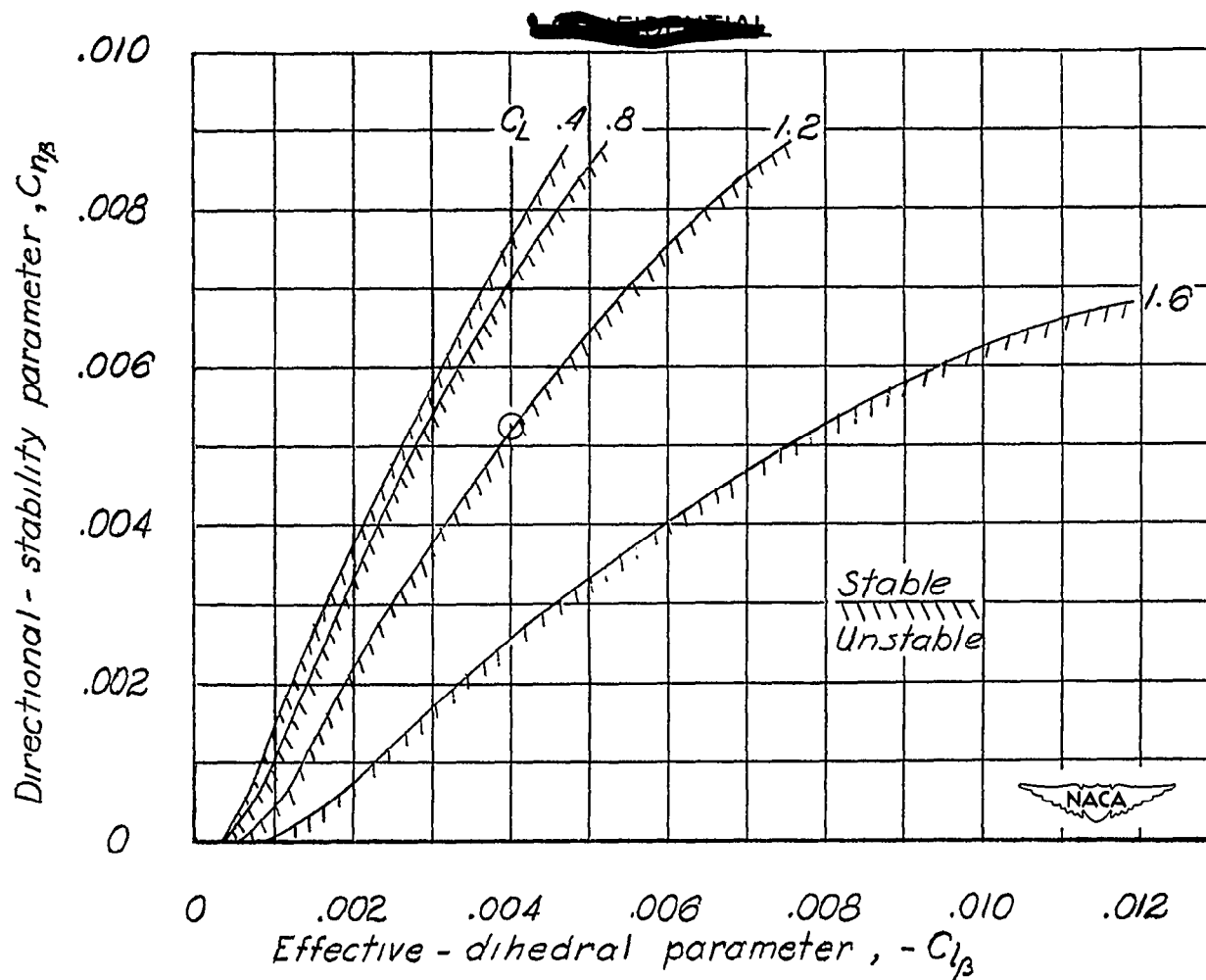


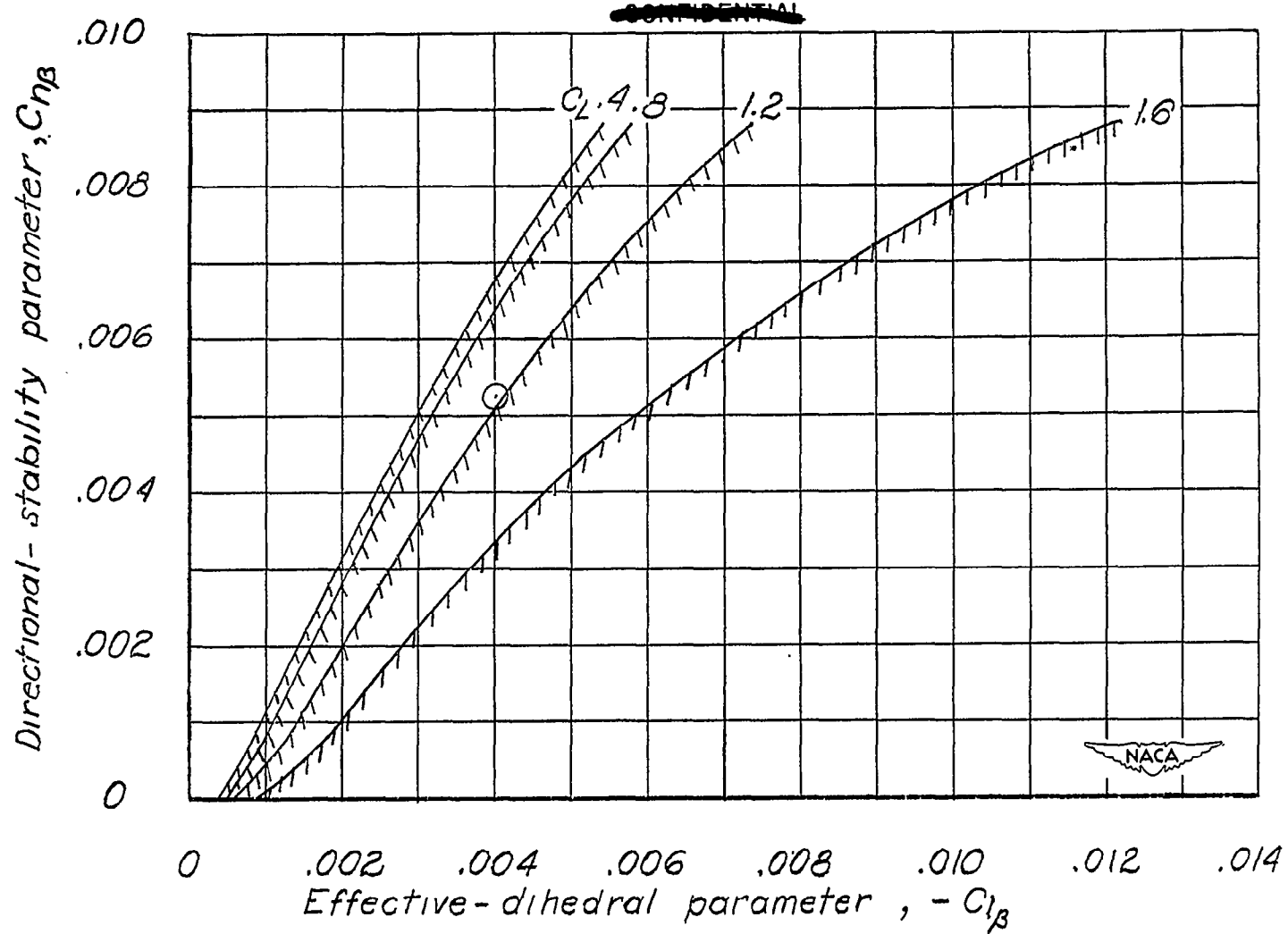
Figure 3.— The stability system of axes. Arrows indicate positive directions of moments, forces, and control-surface deflections. This system of axes is defined as an orthogonal system having their origin at the center of gravity and in which the Z-axis is in the plane of symmetry and perpendicular to the relative wind, the X-axis is in the plane of symmetry and perpendicular to the Z-axis, and the Y-axis is perpendicular to the plane of symmetry.



(a) 53,000 pounds.

Figure 4.— Effect of lift coefficient on the $R = 0$ boundary of the MX-838 airplane.
Flaps 40° ; sea level.

~~CONFIDENTIAL~~



(b) 32,017 pounds.

Figure 4.— Concluded.

~~CONFIDENTIAL~~

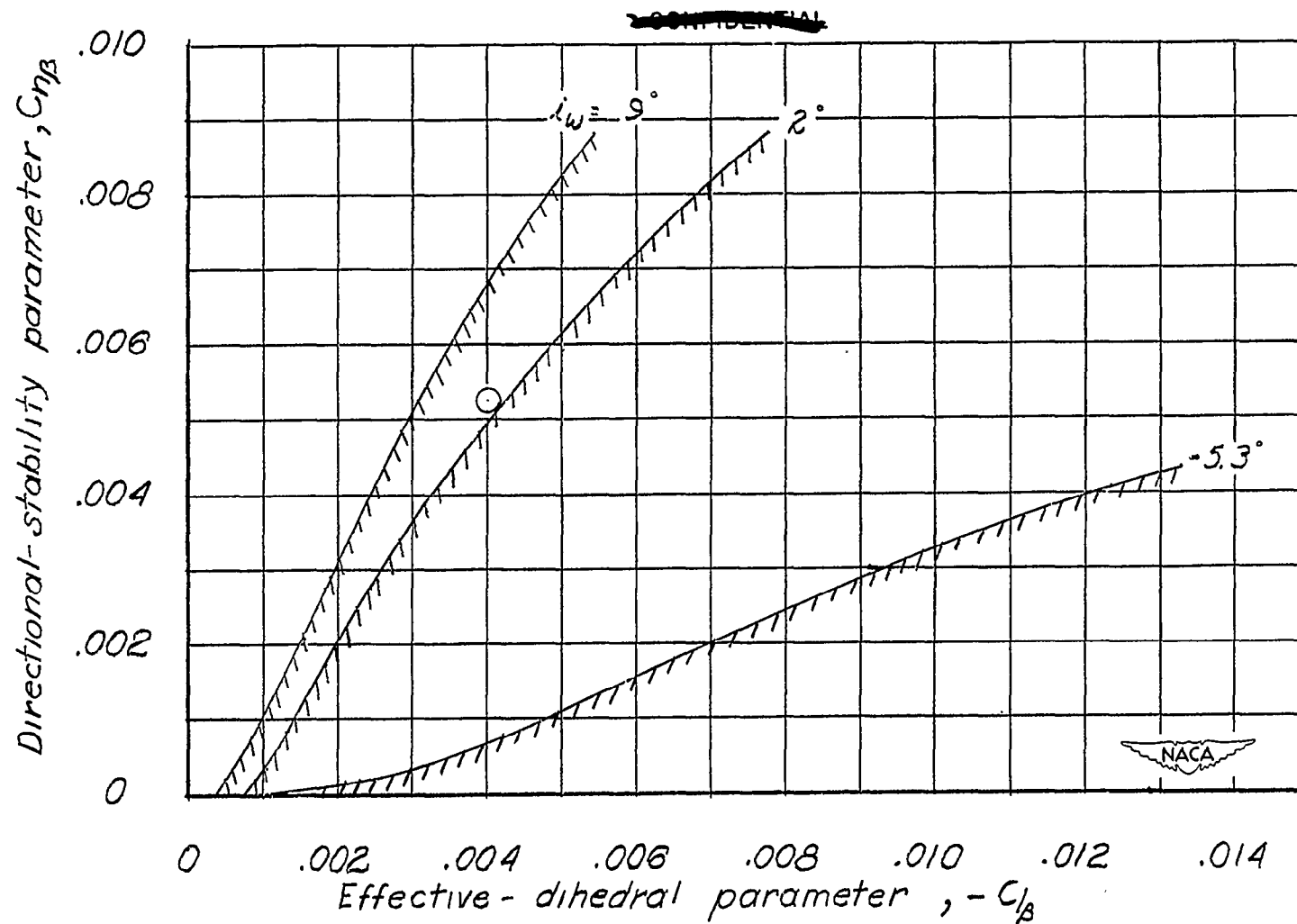
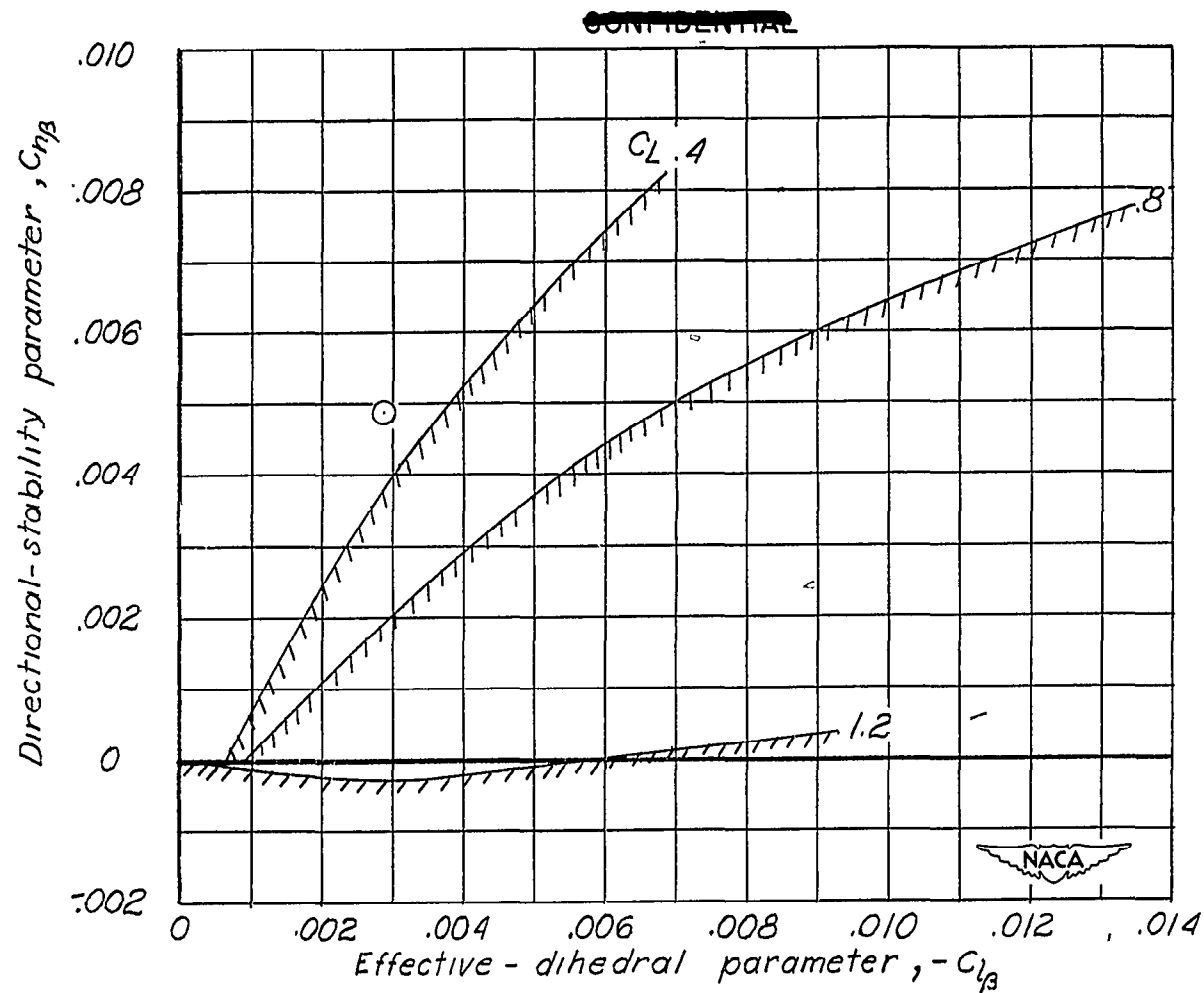


Figure 5.— Effect of wing incidence on the $R = 0$ boundary of the MX-838 airplane. Flaps 40° ; sea level; 32,017 pounds; $C_L = 0.4$.

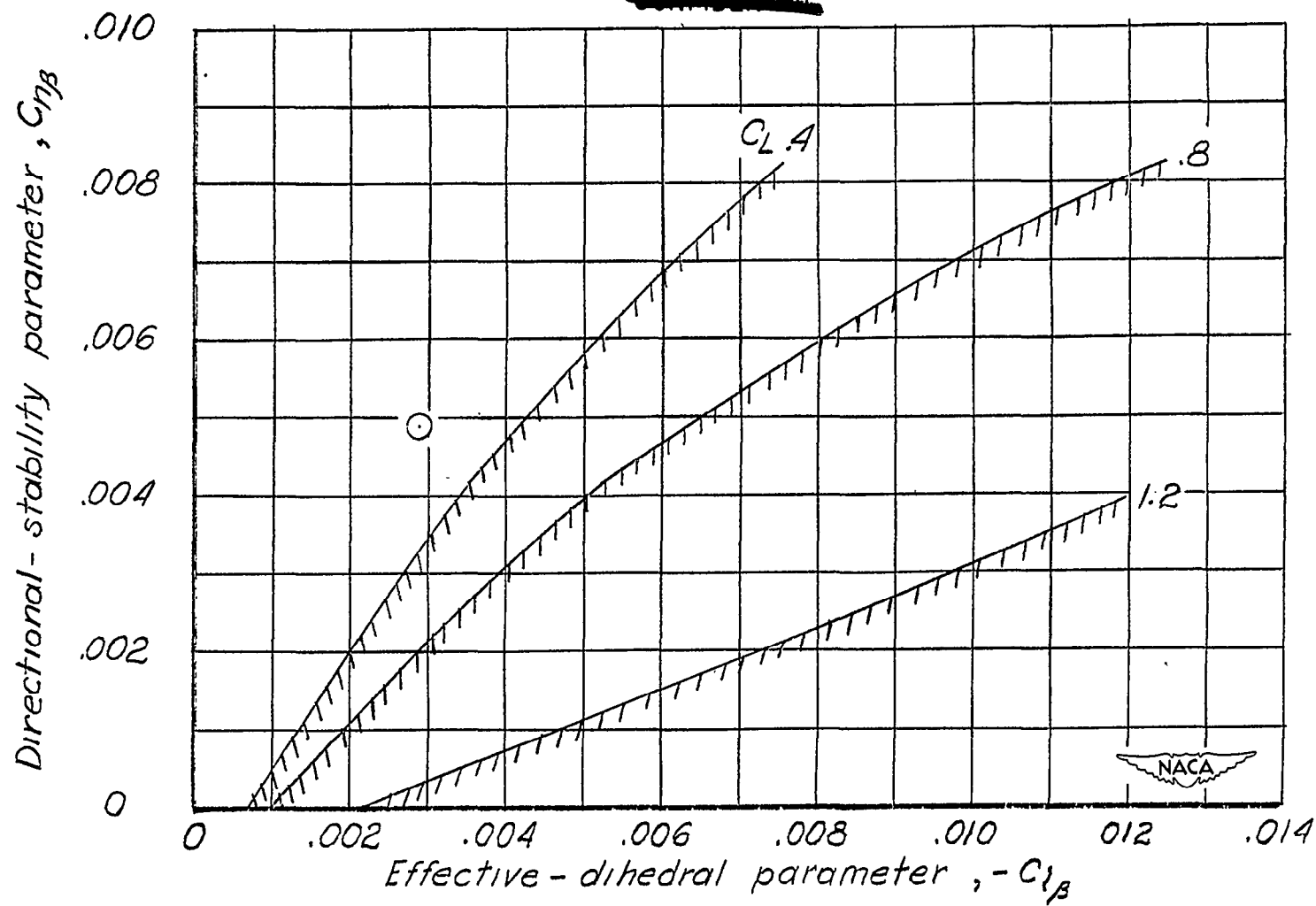
~~CONFIDENTIAL~~



(a) 53,000 pounds.

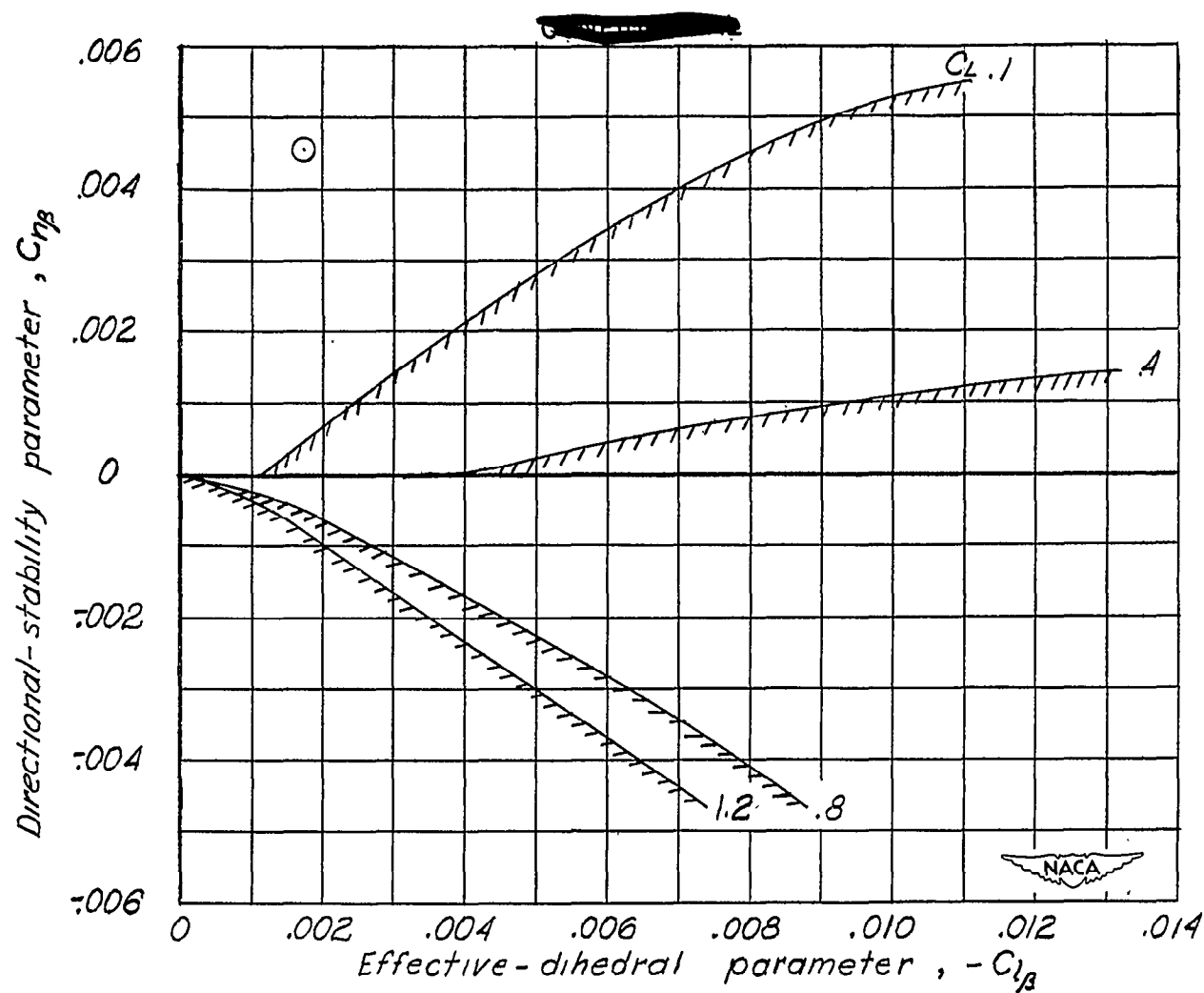
Figure 6.— Effect of lift coefficient on the $R = 0$ boundary of the MX-838 airplane.
Flaps 20° ; sea level.

~~CONFIDENTIAL~~



(b) 32,017 pounds.

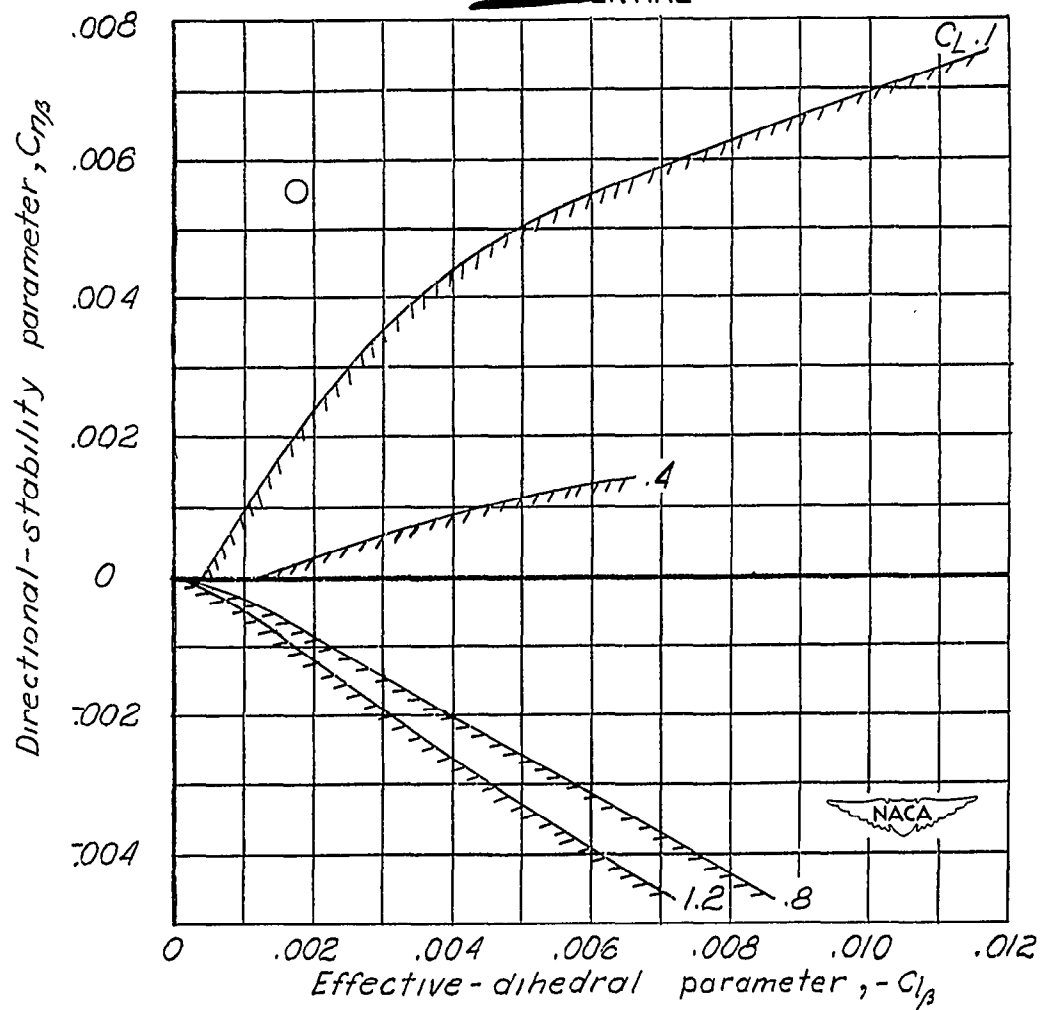
Figure 6.- Concluded.



(a) Sea level.

Figure 7.— Effect of lift coefficient on the $R = 0$ boundary of the MX-838 airplane.
Flaps 0° ; 53,000 pounds.

~~CONFIDENTIAL~~



(b) 35,000 feet.

Figure 7.- Concluded.
~~CONFIDENTIAL~~

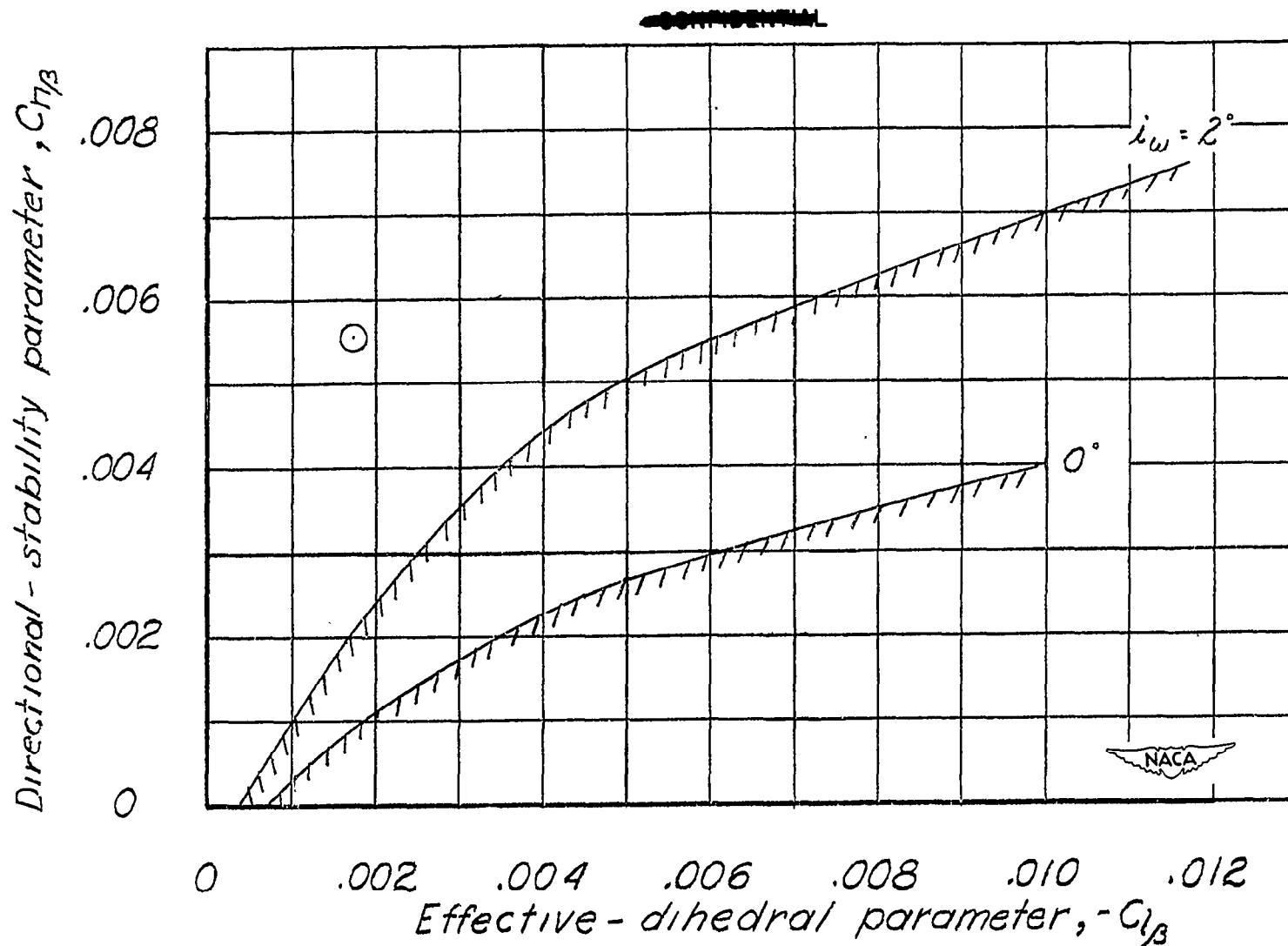


Figure 8.— Effect of wing incidence on the $R = 0$ boundary of the MX-838 airplane. Flaps 0° ; 35,000 feet; 53,000 pounds.

~~CONFIDENTIAL~~

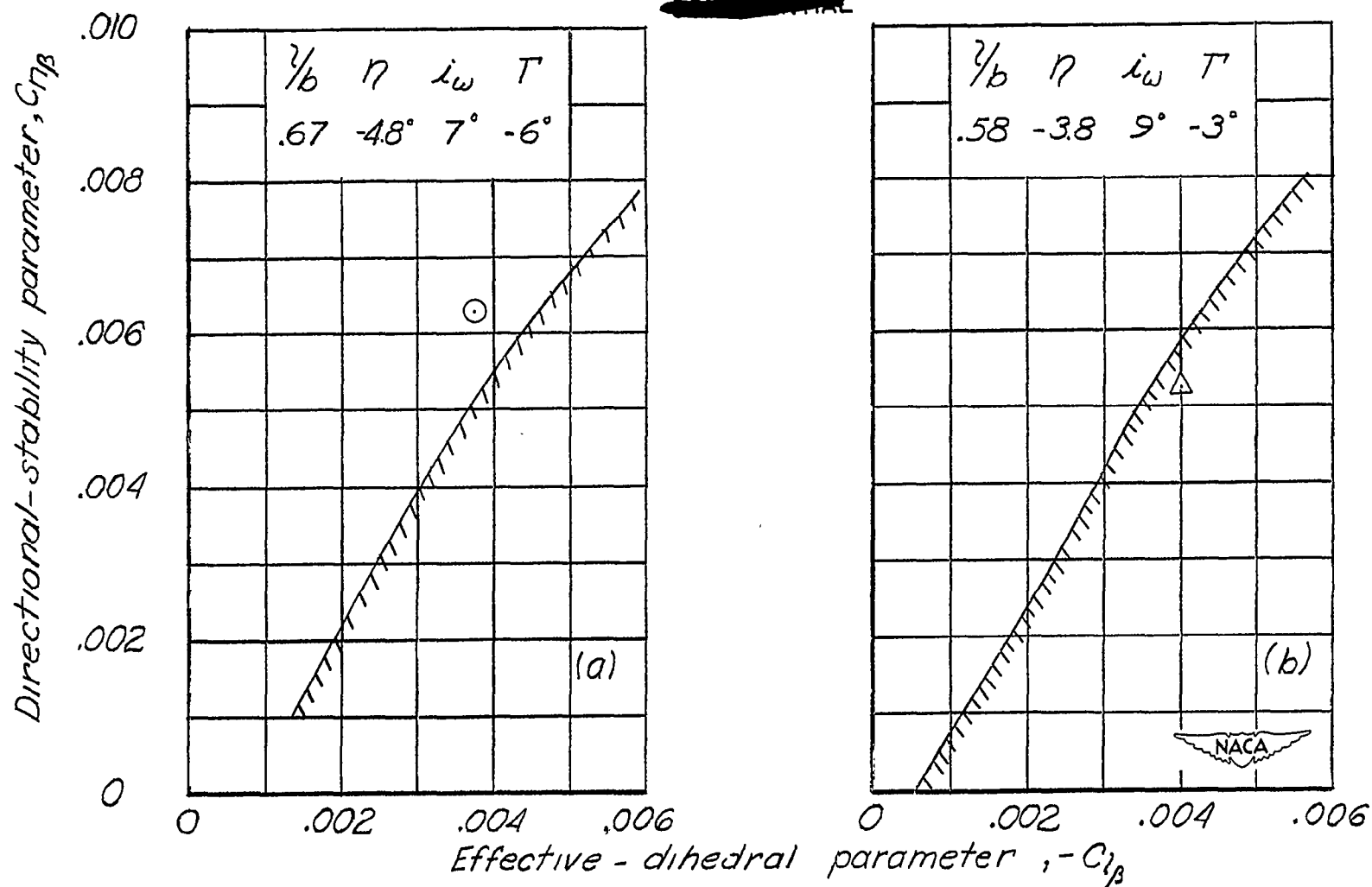


Figure 9.— Effect of modifications to the MK-838 airplane on the $R = 0$ boundary. Flaps 40°; sea level; 40,200 pounds; $C_L = 1.05$.

~~CONFIDENTIAL~~

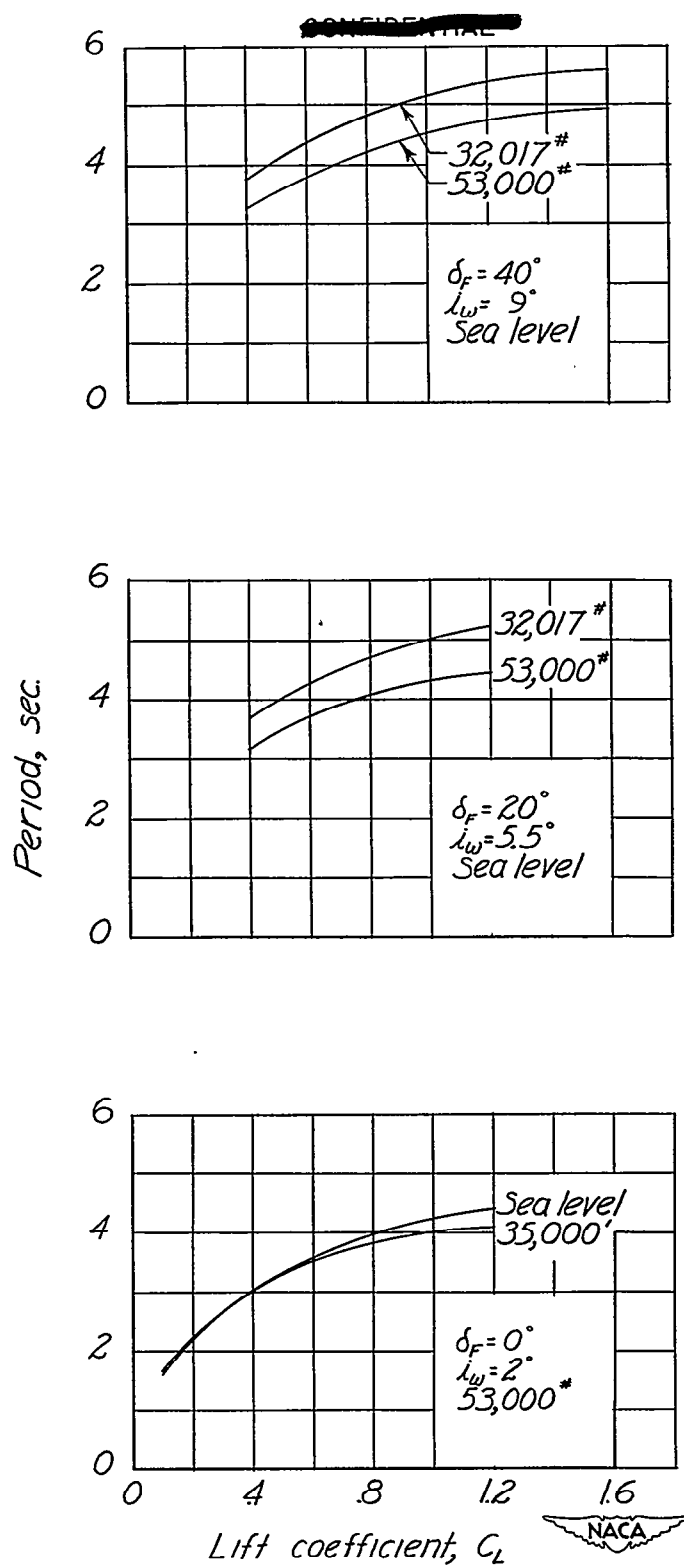


Figure 10.— Period of the lateral oscillation of the MX-838 airplane.

~~CONFIDENTIAL~~

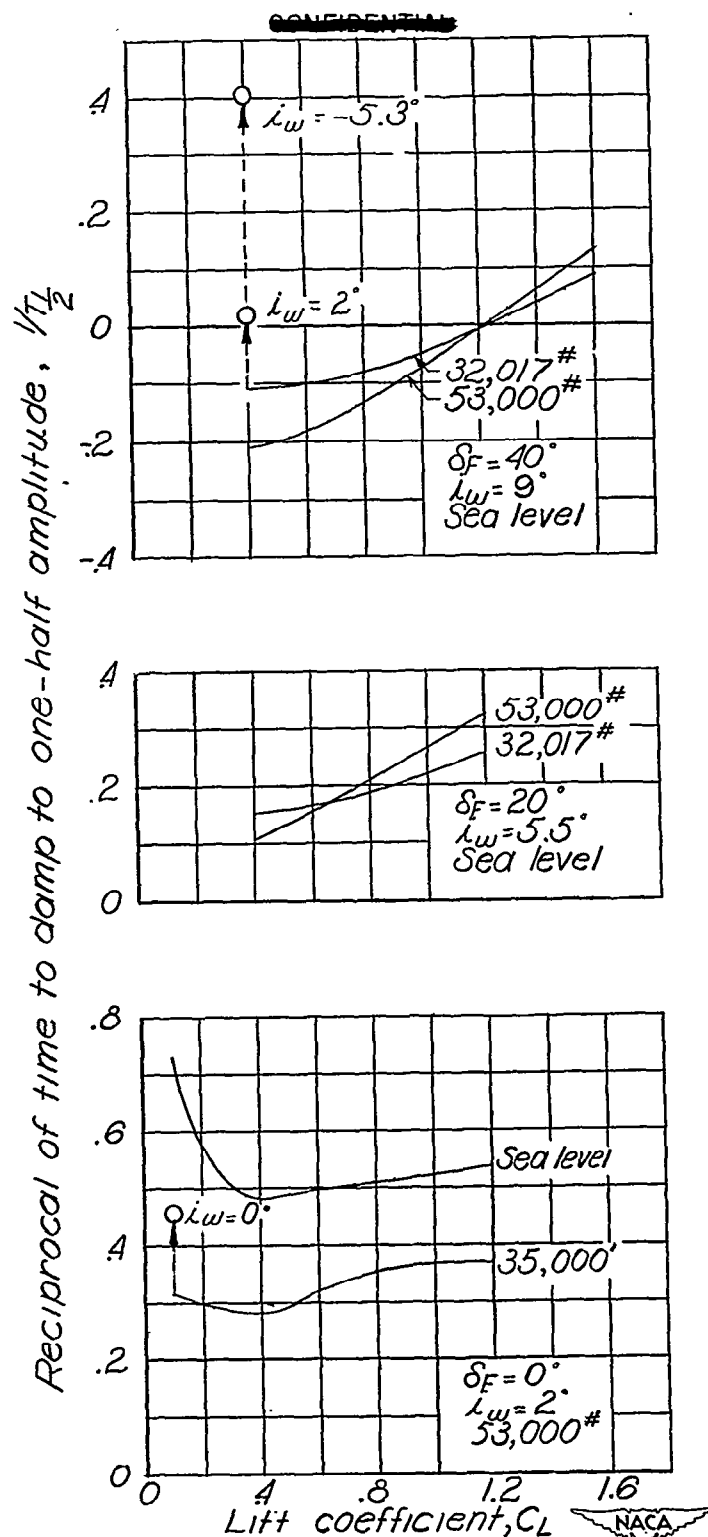


Figure 11.— Damping of the lateral oscillation of the MX-838 airplane in terms of the reciprocal of the time to damp to half amplitude.

~~CONFIDENTIAL~~

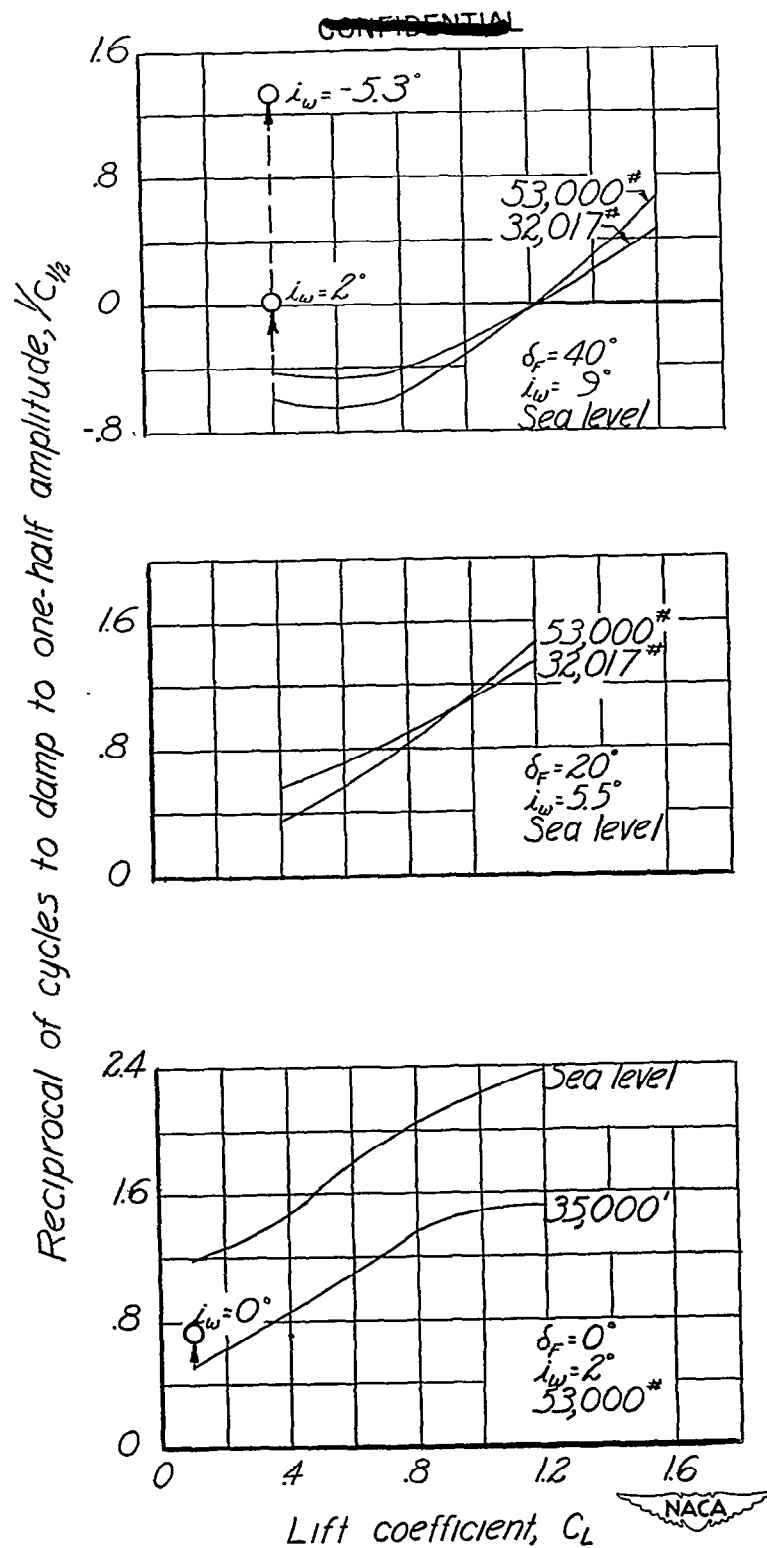


Figure 12.— Damping of the lateral oscillation of the MX-838 airplane in terms of the reciprocal of the cycles to damp to half amplitude.

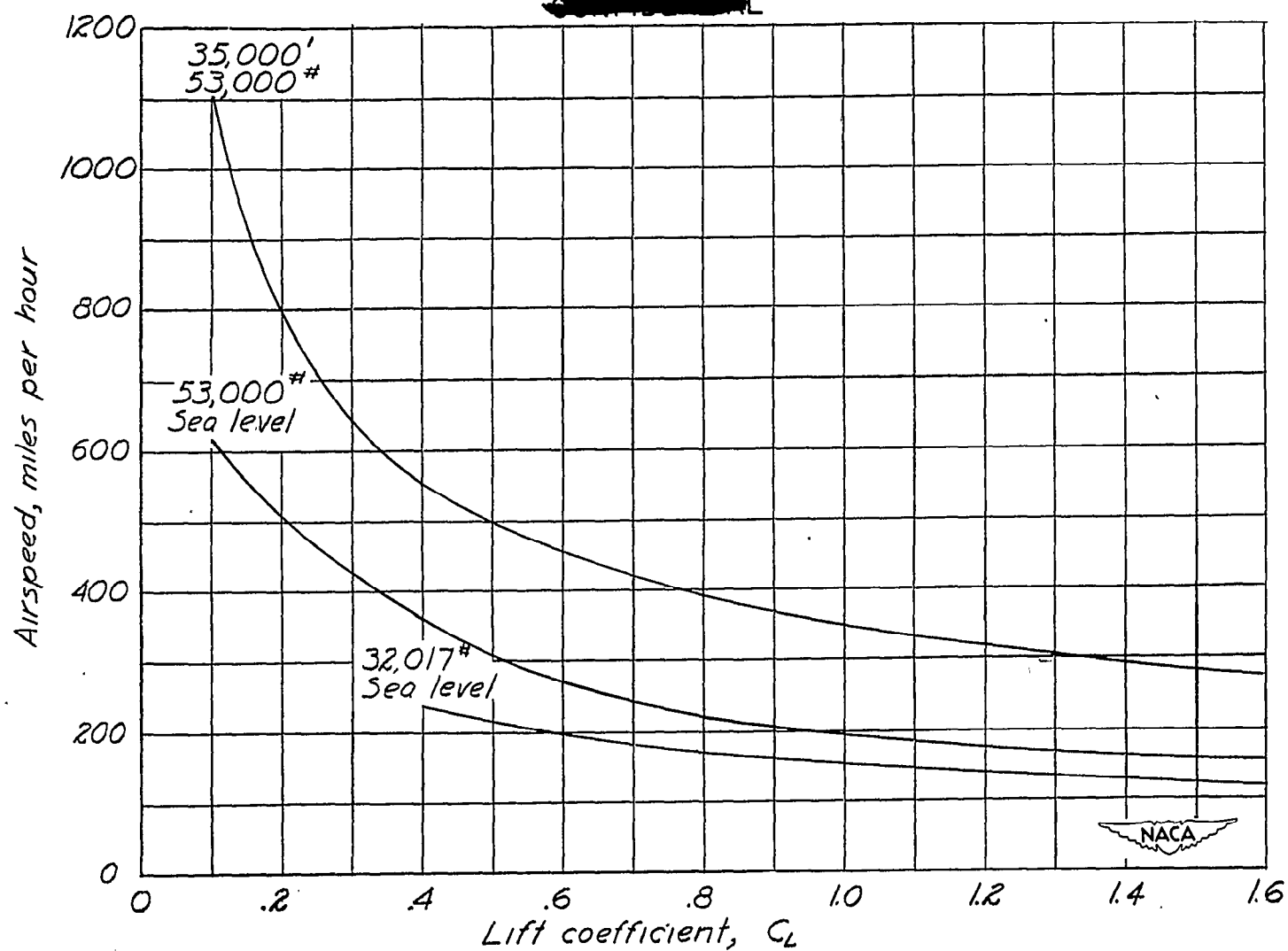


Figure 13.— Effect of altitude and weight on the airspeed required for a given lift coefficient the MX-838 airplane.

~~CONFIDENTIAL~~

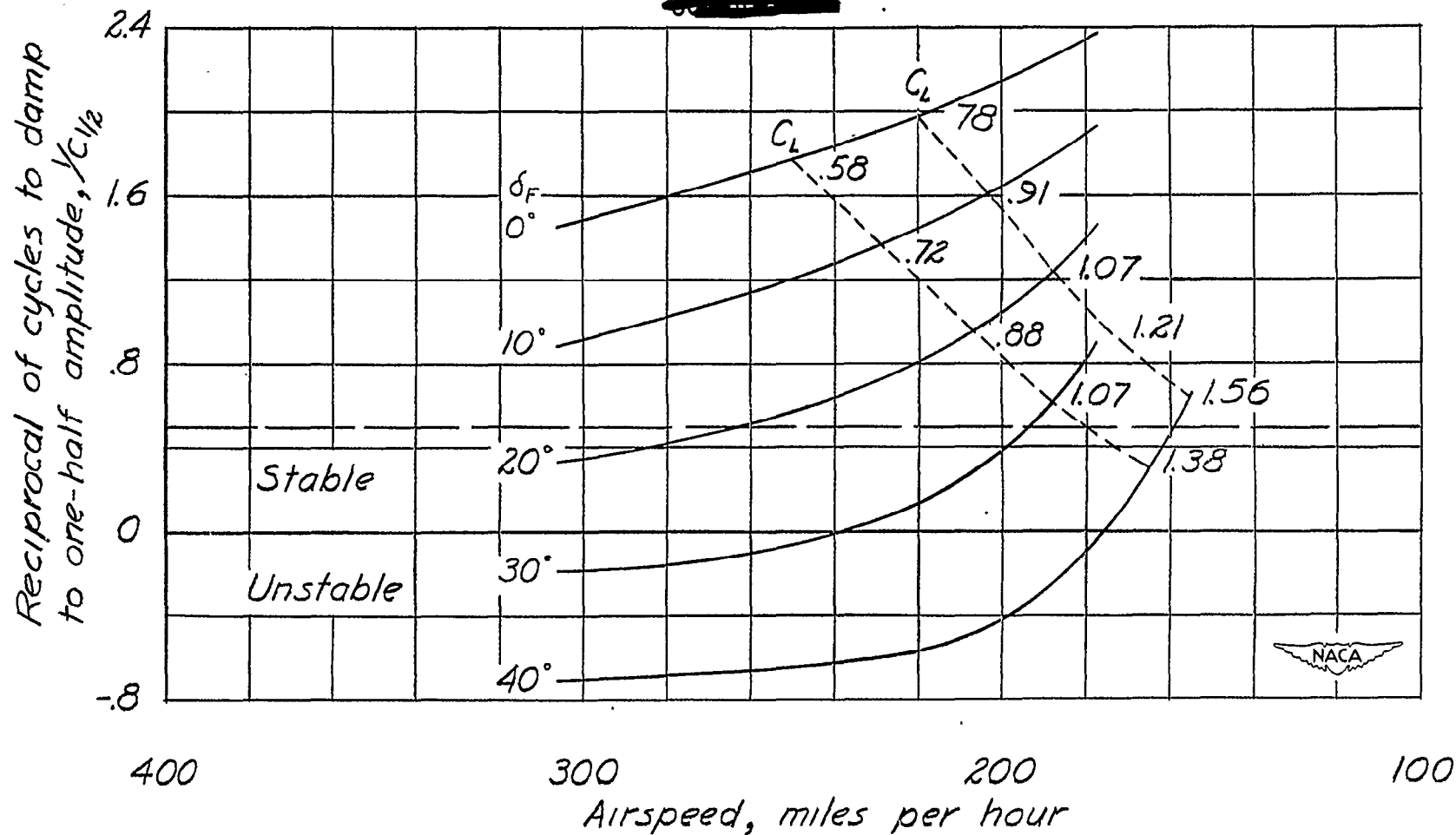


Figure 14.— Design chart showing the effect of flap setting and airspeed on the damping of the lateral oscillation of the MX-838 airplane.

~~CONFIDENTIAL~~

~~CONFIDENTIAL~~

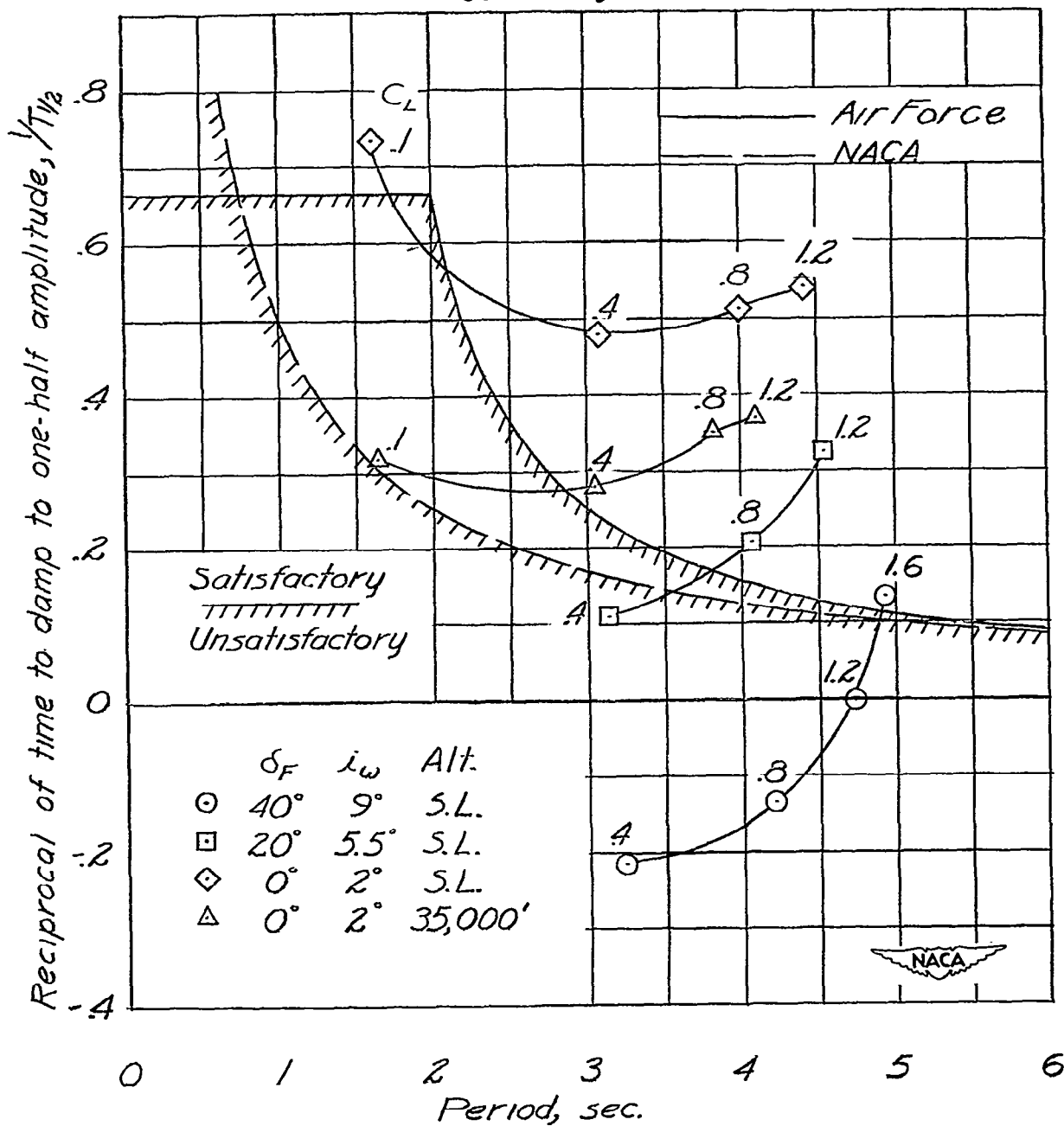


Figure 15.— Comparison of the damping of the MX-838 airplane with respect to the NACA and Air Force requirements. 53,000 pounds.

~~CONFIDENTIAL~~

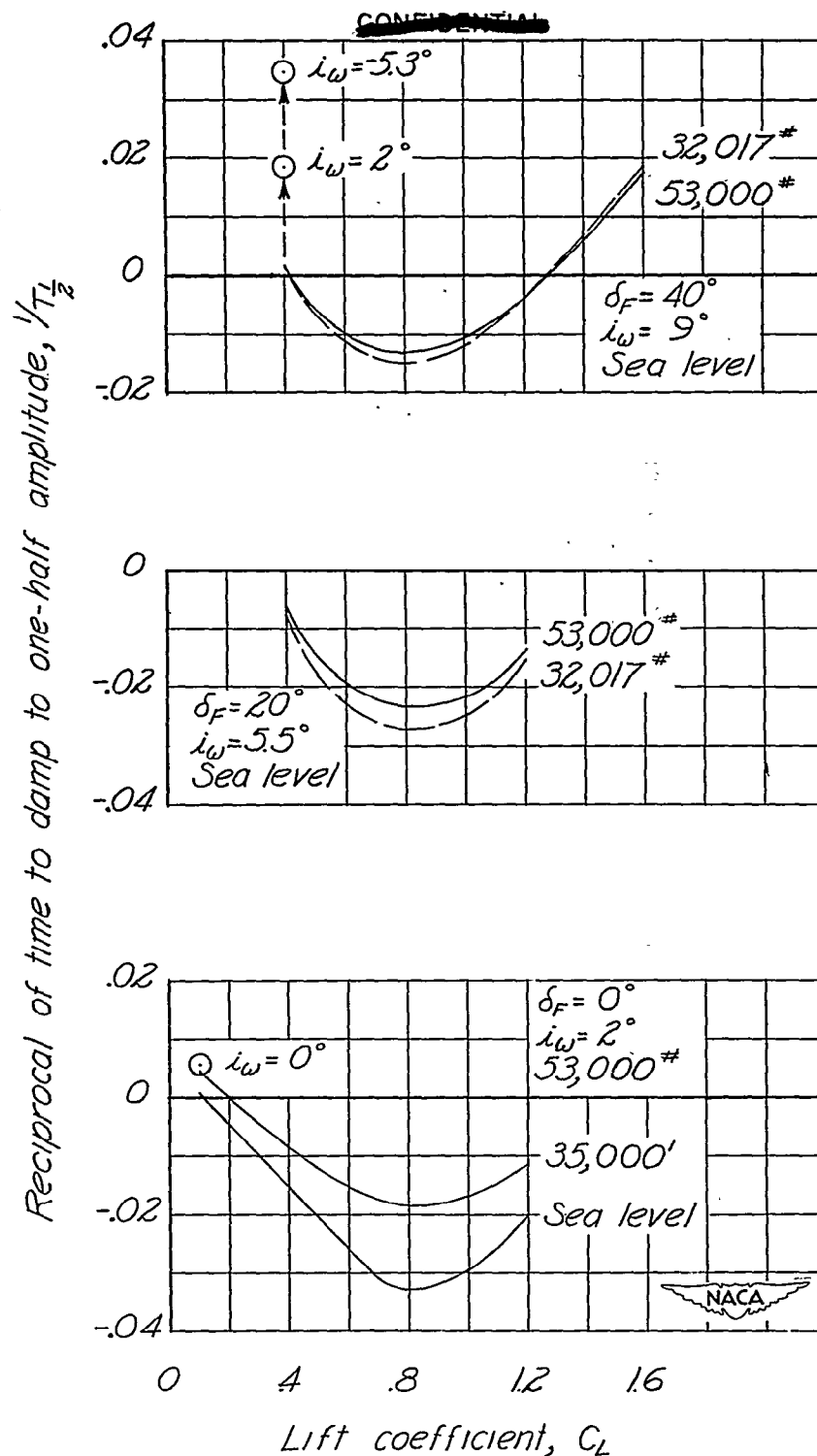


Figure 16.— Damping of the spiral motion of the MX-838 airplane in terms of the reciprocal of the time to damp to one-half amplitude.

~~CONFIDENTIAL~~

